

M Keilhacker  
and the JET Team

# Fusion Physics Progress on JET

"This document is intended for publication in the open literature. It is made available on the understanding that it may not be further circulated and extracts may not be published prior to publication of the original, without the consent of the Publications Officer, JET Joint Undertaking, Abingdon, Oxon, OX14 3EA, UK".

"Enquiries about Copyright and reproduction should be addressed to the Publications Officer, JET Joint Undertaking, Abingdon, Oxon, OX14 3EA".

# Fusion Physics Progress on JET

M Keilhacker and the JET Team.

JET Joint Undertaking, Abingdon, Oxfordshire, OX14 3EA,

Preprint of a Paper accepted for publication in Fusion Engineering and Design

January 1999

## **ABSTRACT**

Twenty years ago the construction of JET began and five years later the first plasma pulses were obtained. A highly successful series of high temperature plasma experiments which addressed all important issues of fusion physics, such as energy confinement, plasma heating and plasma-wall interaction, laid the foundation for a Preliminary Tritium Experiment in 1991, a three stage programme of progressively more closed divertors from 1992 to 1999 and an extended experimental campaign in D-T in autumn 1997. The key physics results from JET are presented, emphasising the synergy between progress in physics and engineering and the impact of the results on improving physics understanding and predictive capability. The physics discussion concentrates on confinement and performance issues in the H-mode and optimised shear regimes, on the development of closed, highly radiating divertors and on the results from the recent broad-based series of D-T experiments. These results include records in fusion performance, the first clear demonstration of alpha particle heating, the testing of ICRF heating scenarios in D-T and the characterisation of the ELMy H-mode in D-T allowing more accurate predictions for the performance of ITER or any other Next Step device.

## **1. INTRODUCTION**

Twenty-five years ago, in 1973, design work on the Joint European Torus (JET) began, five years later, on 1<sup>st</sup> June 1978, the JET Joint Undertaking came into being and construction of the JET device followed, and another five years later, in 1983, the first plasma pulses were obtained. The International Organising Committee of the 1998 SOFT Conference decided to mark these anniversaries of the JET Project with two complementary invited papers: while this paper highlights the progress in fusion physics on JET, the companion paper [1] discusses the technological achievements and experience at JET.

In the following sections the key physics results obtained on JET over the last fifteen years are reviewed, emphasising the interdependence between progress in physics and engineering and highlighting the impact the results had on improving our physics understanding and on defining the Next Step Tokamak, currently seen as the International Thermonuclear Experimental Reactor (ITER) [2].

In this latter context it is important to recall that JET is essentially a one-third scale model of ITER, nearest in size and operating conditions to ITER and with a very similar plasma and divertor configuration. In addition, JET is now the only experiment world-wide able to study fusion power production and fusion physics in deuterium-tritium (D-T). It has also developed a unique capability for remote installation and repair, which was used successfully earlier this year for the planned installation of a new divertor in the activated environment resulting from operation in D-T.

As will be seen in the following discussion, JET's success owes much to its courageous design features (such as non-circular plasma cross-section, high plasma current, and tritium and remote handling capability) and to the general flexibility built into its original design which allowed major modifications and upgrades to be implemented within reasonable time and cost. This teaches an important lesson for the design of ITER or any Next Step machine which has to be capable of operating at the forefront of fusion research for at least twenty-five years after its design has been completed.

The paper is structured in the following way. Section 2 discusses JET results during the early years with limiter and X-point operation (1983-1991) culminating in the Preliminary Tritium Experiment (PTE) in 1991. Section 3 discusses JET's divertor development programme (1992-1999), which is based on a sequence of progressively more "closed" divertors and has the dual objective of providing impurity control and power handling capability for JET and developing a divertor concept for ITER. Section 4 highlights the results of JET's broad-based series of D-T experiments in 1997, including records in fusion performance, the demonstration of alpha particle heating, the testing of ICRF heating scenarios in D-T and the characterisation of the standard operating mode for ITER (steady-state ELMy H-mode) leading to more accurate predictions for ITER performance. Section 5 then addresses JET's contributions to more advanced tokamak scenarios, namely the discovery of the Pellet-Enhanced Performance (PEP)-mode in 1988 and the work on the optimised shear mode (since 1996). A summary and conclusions follow in Section 6.

## **2. LIMITER AND X-POINT OPERATION (1983-1991)**

### **2.1 Basic limiter machine (1983-1986)**

JET was originally conceived as a limiter tokamak featuring, first, toroidally discrete and then continuous ("belt") limiters. First operation (1983-1984) with ohmic heating showed already that the large volume, high current JET plasmas were capable of sustaining reactor grade energy confinement times ( $\sim 1$ s). The addition of strong ICRF and NB heating (1984-1986) also allowed reactor temperatures ( $\sim 12$ keV) to be achieved, but at the same time demonstrated the degradation of energy confinement time,  $\tau_E$ , with increasing heating power,  $P$  (Fig. 1(a)) [3]. The JET results confirmed the scaling  $\tau_E \sim I_p P^{-0.5}$  (Goldston scaling [4]) found on smaller tokamaks and extended it to plasma currents in the Megaampere and heating powers in the Megawatt range. After the discovery of the H-mode in ASDEX in 1983 [5], X-point operation (not originally foreseen on JET) in 1986 allowed the first demonstration of H-mode confinement in a large tokamak (Fig. 1(a)) [6]. Carbon dump plates attached inside the vessel at the top and the bottom were used and plasmas with currents up to 3MA were studied.

## 2.2 Upgraded machine (1986-1991)

The period 1986 - 1988 saw major upgrades of the JET power supply systems to allow even higher plasma currents in both limiter and X-point operation. This resulted in limiter operation up to 7.1MA (well above the 4.8MA design limit) and X-point operation up to 5.1MA (single null) and 4.5MA (double null) (Fig. 1(b)).

With these upgrades it could be shown that even with strong additional heating, required to push plasma temperatures into the reactor regime, high current H-mode operation allows reactor grade energy confinement times ( $\sim 1$ s). These JET results had a major impact on the world tokamak programme: the reactor design of NET in Europe was reviewed, leading to a substantial increase in the plasma current to 20MA, and the subsequent design of ITER settled for a plasma current of 21-24MA [2].

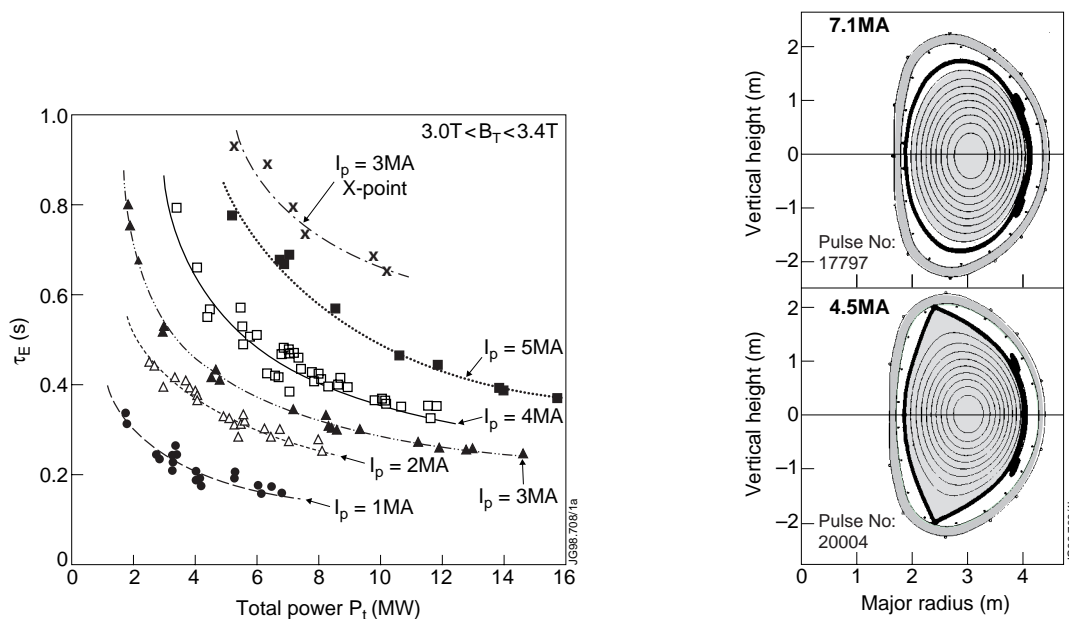


Fig. 1 (a) Energy confinement time versus total heating power for 1 to 5 MA limiter and 3MA X-point discharges, and (b) 7.1MA limiter and 4.5MA double null X-point configurations.

To reduce the effective ionic charge  $Z_{\text{eff}}$ , JET finally (1988-1991) changed to low Z (carbon, beryllium) plasma facing components and to beryllium evaporation onto the vessel walls between pulses. This reduced  $Z_{\text{eff}}$  and brought a further improvement in JET performance resulting, albeit transiently (Section 3), in a fusion triple product  $n_{i0}\tau_E T_{i0}$  of  $9 \times 10^{20} \text{ m}^{-3} \text{ s keV}$  [7,8] which is only a factor of 6 short of ignition and, if reproduced in D-T, would correspond to breakeven.

## 2.3 Preliminary Tritium Experiment (1991)

With these upgrades, JET performance had reached the level which warranted the use of tritium for the first time in a laboratory plasma experiment and the so-called Preliminary Tritium Experiment (PTE) was carried out in November 1991. To limit the activation of the machine so that

the extensive in-vessel re-construction which was planned to follow the PTE could still be carried out, only 10% of tritium in deuterium was used and only two pulses were carried out. These two pulses were very similar, each producing a peak fusion power of 1.7MW, averaging 1MW over a 2 second period (Fig. 2) [8]. This was the world's first controlled production of significant fusion power and had a big impact on the public perception of nuclear fusion.

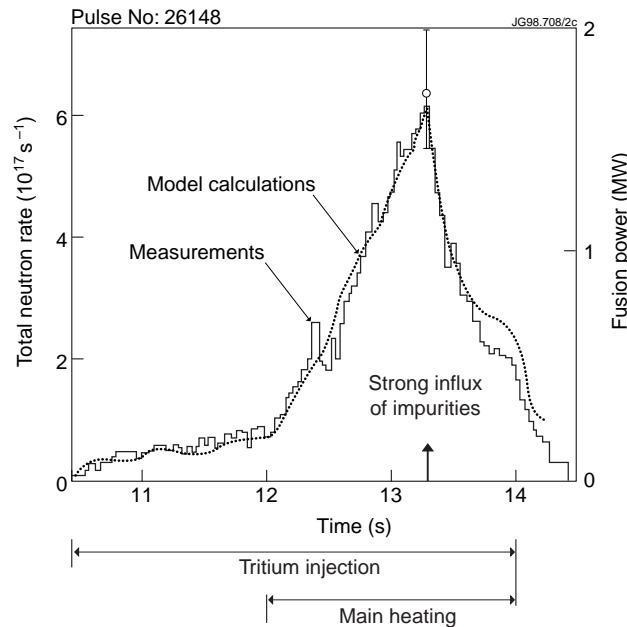
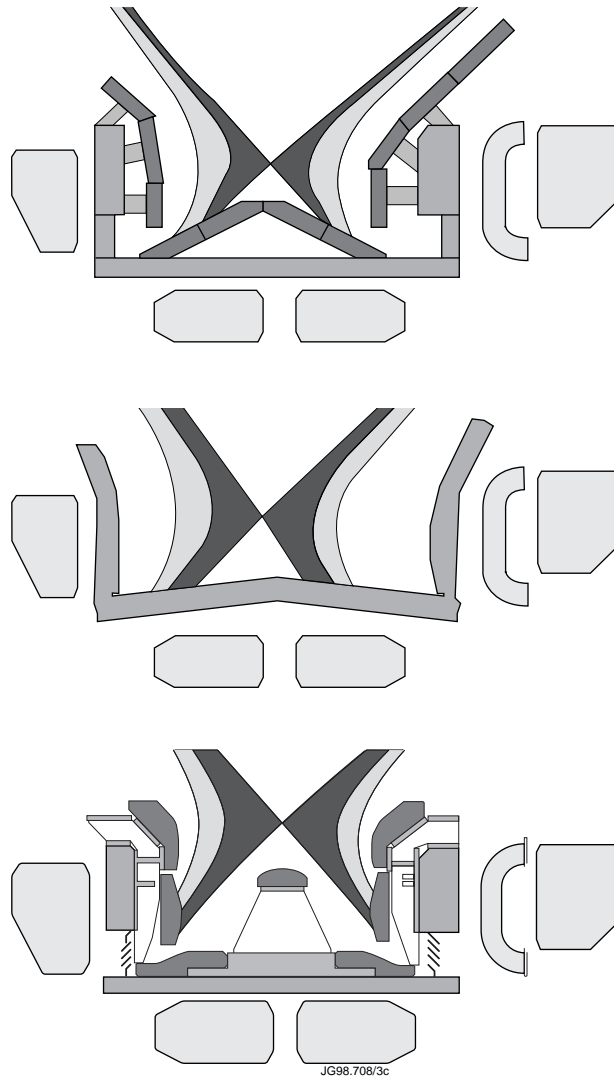


Fig. 2 Measured and calculated (TRANSP simulation) total neutron rate (predominantly 14MeV neutrons) for one of the two PTE pulses.

### 3. DIVERTOR CONCEPT DEVELOPMENT (1992-1999)

In the PTE discharges - as in similar discharges in D-D - the high performance phase was terminated after 1 to 2 seconds by magneto-hydrodynamic instabilities which led to overheating of the target plates and large influxes of carbon (carbon “bloom”) (Fig. 2). This prompted JET to embark on a divertor programme with the dual objective of controlling the impurity influxes in JET and, more generally, of developing a divertor concept for ITER. The divertor concept under consideration was that of a “radiative” divertor [9], in which charge exchange and radiative power losses throughout the divertor volume reduced the heat load to the target plates, finally leading to “detachment” of the plasma from the targets and to reduced physical sputtering and erosion of the targets. JET devised and carried out a three stage programme of progressively more “closed” divertors (Fig.3) [10] which were expected to provide easier access to radiative/detached regimes, to increase divertor neutral pressure and pumping (particularly for helium exhaust in a reactor) and to reduce the core plasma impurity content by lowering the main chamber neutral pressure and increasing the retention of target produced impurities.



*Fig. 3 Schematic poloidal cross-sections of the progressively more closed Mark I, Mark IIA and Mark IIGB divertors.*

### **3.1 Effect of divertor closure on divertor and global performance**

Comparison of results from the more open Mark I and more closed Mark IIA divertors shows [11] that, as predicted, detachment occurs at lower upstream densities for a fixed power (Fig. 4(a)) and the neutral pressure at the pump increases (Fig. 4 (b)) leading to increased pumping. Also, as predicted, the main chamber neutral pressure decreases with increasing closure; however, confinement was unchanged (Fig. 5) [11].

Contrary to expectations, it was found that the core plasma impurity content ( $Z_{\text{eff}}$ ) was practically unaffected by the divertor closure (Fig. 6) [12], even though the main chamber neutral pressure and the corresponding wall sputtering were lower in the more closed Mark IIA/AP divertor. One reason for this is a higher observed impurity production from the Mark IIA/AP divertor targets which is attributed to an increased chemical sputtering yield at their higher



target temperatures ( $\sim 500^\circ\text{K}$  in Mark IIA/AP compared to  $\sim 300^\circ\text{K}$  in Mark I). It may also suggest that the vessel walls/baffles rather than the divertor targets are the dominant source of impurities.

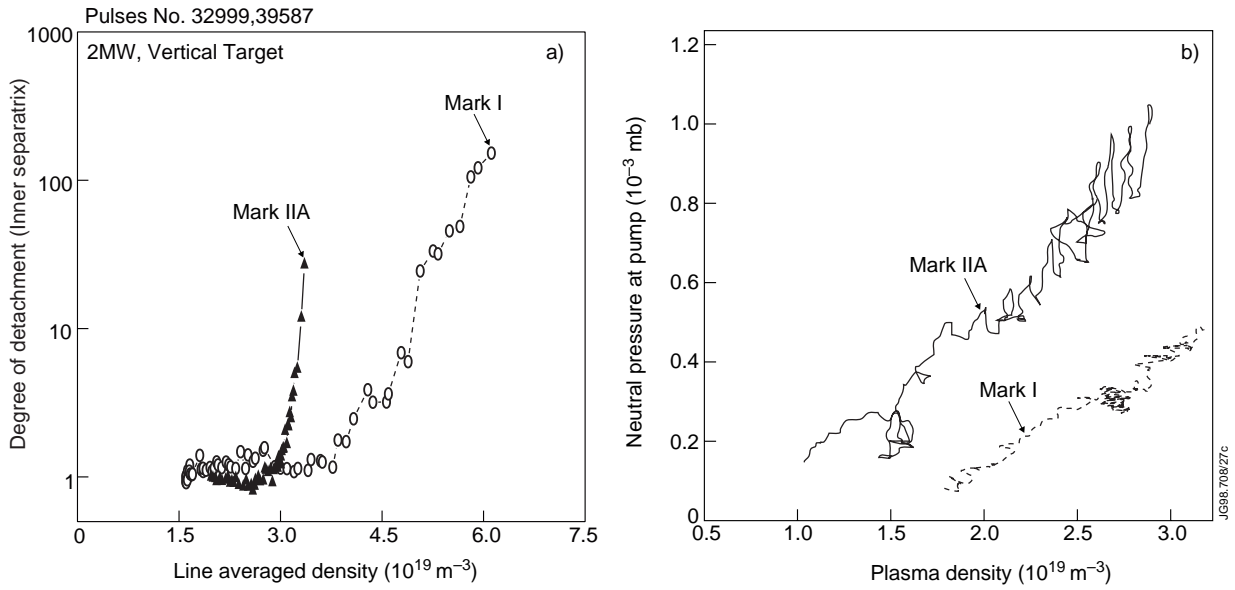


Fig. 4 Comparison of (a) inner divertor detachment for two vertical target L-mode discharges, and (b) subdivertor pressure (proportional to pumping speed) for two Ohmic discharges, in the Mark I and Mark IIA divertors.

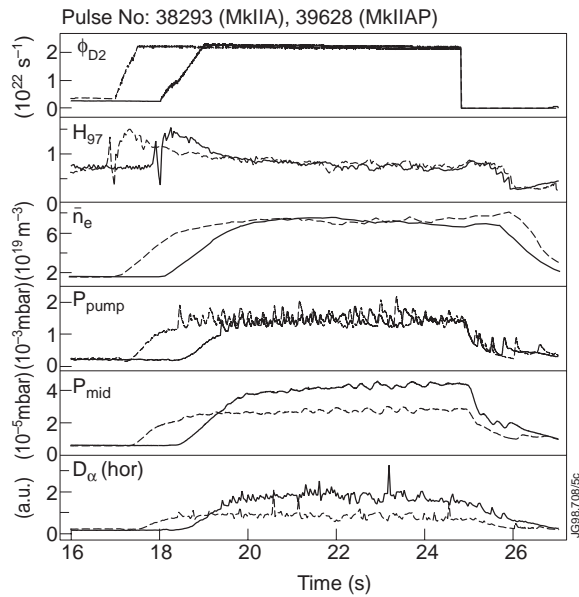


Fig. 5 Comparison of main chamber neutral pressure ( $P_{\text{mid}}$ ) and energy confinement quality factor ( $H_{97}$ ) in the Mark IIA and Mark IIAP divertors.

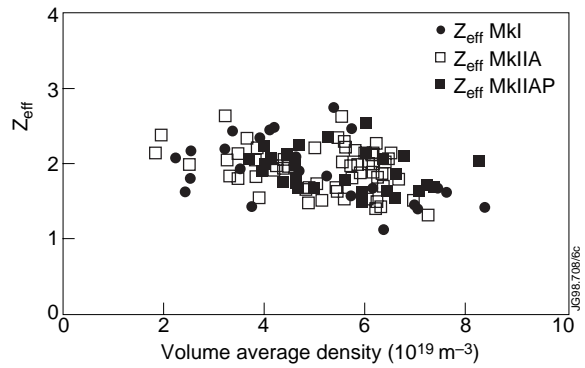


Fig. 6 Comparison of core plasma impurity content ( $Z_{\text{eff}}$ ) in the Mark I, Mark IIA and Mark IIAP divertors.

At first sight, the H-mode power threshold and the density limit are little affected by the divertor configuration [11]. However, closer examination of the H-mode power threshold database shows that the threshold is somewhat lower in the more closed Mark IIA divertor and even lower with plugged neutral leakage paths (Mark IIAP).

### 3.2 Compatibility between plasma and divertor performance and extrapolation to ITER

As can be seen from Fig. 7, energy confinement degrades as high density is approached with gas fuelling (at about 80% of the Greenwald density limit,  $n_{GW}$ [13]), and at high radiative power fraction ( $f_{rad}>0.5$ ) with impurity seeding [14]. This shows that the final aim of a coherent scenario combining a radiative divertor and a reactor-grade plasma core is still not quite achieved. To exemplify this, Table I compares the ITER requirements [15] with what has been obtained so far. It can be seen, that most requirements have been met, except for the relatively low density limit and, in particular, the degradation of confinement to 80% of the ITERH-97(y) scaling expectations at 80% of the density limit. The situation might be recovered if the density is increased by the injection of deuterium ice pellets with deeper fuelling than is obtained with gas puffing. After encouraging results on ASDEX-UG [16], the effect of deep fuelling using inboard (high magnetic field side) pellet injection will be studied by JET in 1999.

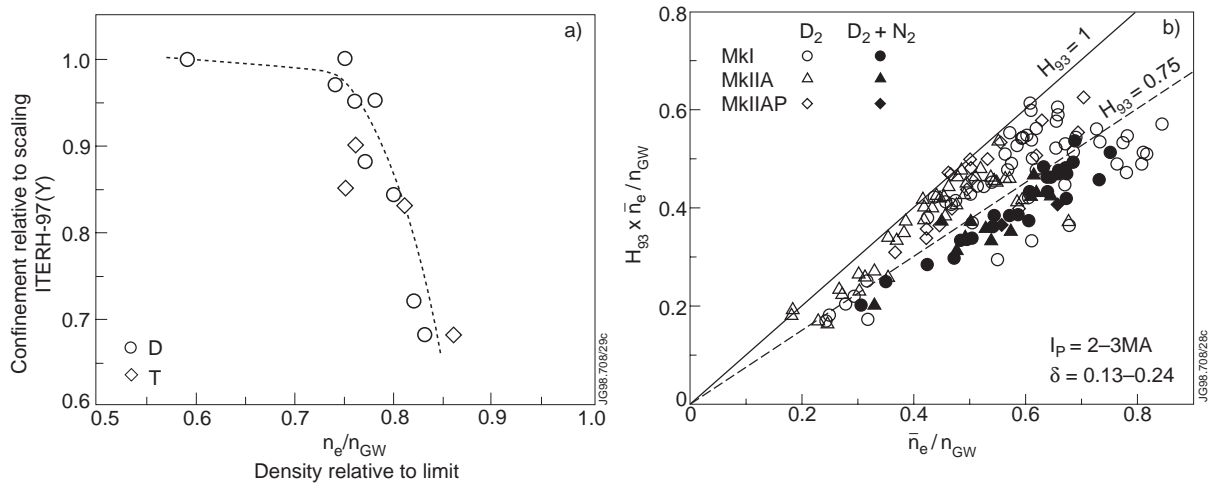


Fig. 7 (a) Energy confinement time relative to ITERH-97(y) scaling versus density relative to Greenwald density, and (b) comparison of the figure of merit  $H_{93} \bar{n}_e/n_{GW}$  for  $D_2$  fuelled and nitrogen seeded radiative discharges with  $f_{rad} > 0.5$  for Mark I, Mark IIA and Mark IIAP.

Table I: Comparison of ITER requirements with what has been achieved so far

ITER Requirements	Status
$H_{97} > 0.8$	achieved with Type I ELMs
$n/n_{GW} > 1.2$	confinement degrades for $n/n_{GW} > 0.8$
$f_{rad} = \frac{P_{rad}}{P_{heat} - P_{brems}} > 0.75$	achieved in seeded radiating discharges
$Z_{eff}$ (excluding He) $< 1.6$	scaled values within scatter of experimental data
$\tau_{He}/\tau_E < 5$	achieved; He concentration determined by exhaust rate

### 3.3 First results with the Mark II Gas Box divertor

The third and most closed of the JET divertors, the Mark IIGB (Gas Box), has been designed to allow more balanced detachment in the two divertor legs (Mark IIGB features a septum which separates the inner and outer divertor regions, and provides for the possibility of differential gas puffing). First results are very encouraging: using fuelling into the outer divertor only, it has been possible in L-mode discharges to produce relatively symmetric ion fluxes to the two divertors resulting in symmetric detachment and an increase in the density limit by almost 20% (Fig. 8) [17]. Similar trends are seen in the distribution of energy deposited to the inner and outer strike zones. These results are very important for ITER and more extensive studies are under way.

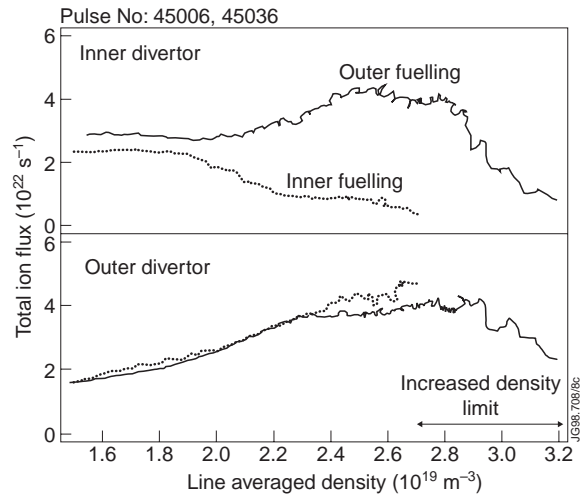


Fig. 8 Fuelling through the outer divertor (rather than the inner) results in more symmetric detachment and an increase in density limit with the Mark IIGB divertor.

## 4. D-T PERFORMANCE AND RELATED PHYSICS (1997)

JET was designed from the outset for D-T operation and uses comprehensive tritium processing and remote handling systems [1]. After the D-T pulses of the PTE in 1991 [8], JET resumed D-T operation in 1997 (from May to June and from September to November) with a broad-based series of D-T experiments (DTE1) which addressed specific questions relating to D-T physics and technology for ITER. The following summarises the most important results of DTE1 (a more detailed discussion can be found in [18] and [19]).

### 4.1 Fusion performance

The hot ion ELM-free H-mode is the traditional mode for the highest, albeit transient, performance [20] and, during DTE1, has led to records of fusion power and  $Q$ . Figure 9 shows the pulse with the highest fusion power of 16.1MW (a similar pulse on the same day one hour earlier produced 15.8MW), which was obtained with 25.4MW of additional heating (22.3MW NB and 3.1MW ICRF heating). The fusion power rises monotonically with time while the ion temperature levels off around 28keV, significantly higher than the electron temperature which is about 14keV. The ELM-free period is limited by MHD activity (as seen in the structure of the Balmer alpha signal): first an outer mode and then a giant ELM which terminates the high performance phase [21]. Following detection of the giant ELM, the heating power is switched off to save neutrons. As shown in the lowest panel of Fig. 9, this pulse reaches record values of the ratios of fusion power to total input power,  $Q_{in}=P_{fus}/P_{in}=0.62$ , and fusion power to total loss power,

$Q_{\text{tot}} = P_{\text{fus}} / (P_{\text{loss}} - P_{\alpha}) = 0.95 \pm 0.17$ , the value which  $Q_{\text{in}}$  would reach if the same plasma conditions could be achieved in steady-state. In the last expression,  $P_{\alpha}$  is the heating by alpha particles taking account of their slowing down process.

In addition, a thorough comparison of similar D-T and D-D H-mode discharges has validated the factor of 210 between D-D and D-T fusion power expected from the respective reaction rate coefficients [22]. This is a very important confirmation that the expected fusion performance can be achieved in D-T.

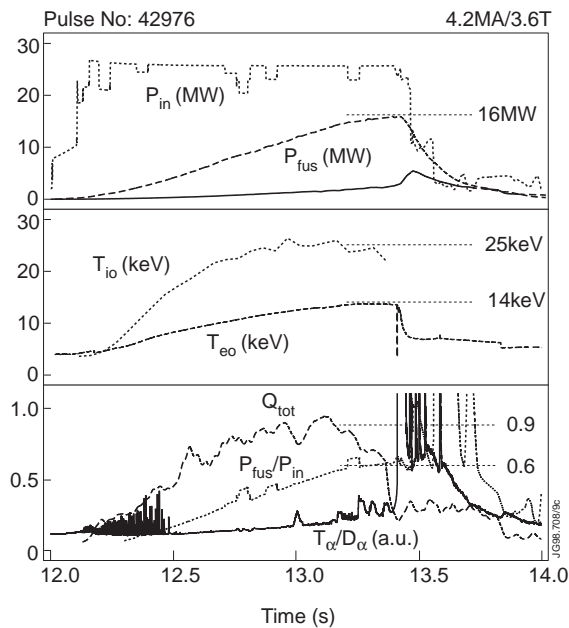


Fig. 9 Various time traces for the highest fusion yield hot-ion H-mode discharge. From top to bottom: Input and fusion power; central ion and electron temperature; ratio of fusion to loss power,  $Q_{\text{tot}}$ , and of fusion to input power,  $Q_{\text{in}}$ , and  $D_{\alpha}/T_{\alpha}$  intensity.

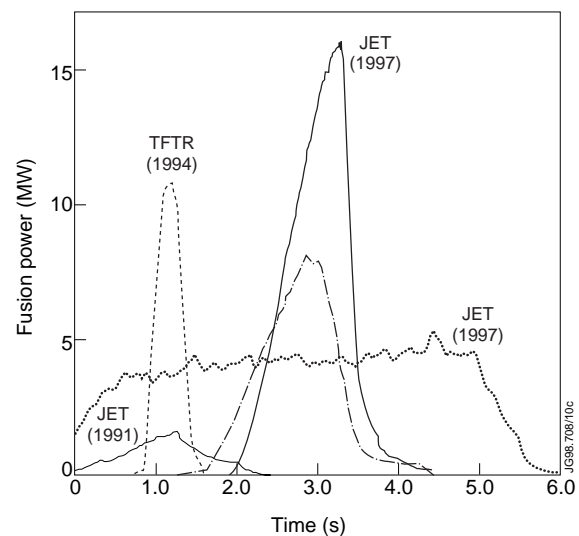


Fig.10 Fusion power development in JET (1991 and 1997) and TFTR (1994). For easier comparison the time point  $t=0$  for these pulses is arbitrary.

Figure 10 summarises the development of fusion power over the last six years in JET and TFTR. It encompasses the first ever high fusion power (1.7MW) pulse with 11% tritium in JET in 1991 [8], the pulse with the highest fusion power (10.7MW) from the 50:50 D-T experiments on TFTR [23] during the period 1993 to 1997, and finally the record pulses from the JET D-T experiments in 1997: 16.1MW, transiently, in an ELM-free H-mode [19], 8.2MW in the optimised shear mode of operation [19] (Section 5), and 4MW in a steady-state ELMy H-mode discharge [24]. In all, a total of 675 MJ of fusion energy was produced during DTE1.

#### 4.2 Alpha particle confinement and heating

One of the most important objectives of the JET high performance D-T experiments was an unambiguous demonstration of alpha particle heating. To separate the alpha particle heating from possible isotope effects on energy confinement, a series of specially designed hot ion ELM-free H-mode pulses was carried out in which the D-T mixture was varied from pure

deuterium to almost pure tritium while all other parameters, including the external heating power ( $\approx 10.5\text{MW}$  NB heating), were kept constant [25]. Comparing the pure deuterium and almost pure tritium ends of this scan demonstrated (lower panel in Fig.11) that the global energy confinement time in ELM-free H-modes has no or only a very weak isotope dependence. The strong correlation between the maximum diamagnetic and thermal plasma energies and the optimum D-T mixture (upper panel in Fig. 11), is a clear demonstration of alpha particle heating. This is seen even more clearly in Fig 12, which is a plot of the central electron temperature versus the calculated alpha particle heating power for the set of pulses in the D-T mixture scan. The highest electron temperature shows a clear correlation with the maximum alpha particle heating power and with the optimum D-T plasma mixture (40:60). A regression fit to the data gives a change in central electron temperature of  $1.3\pm 0.23\text{keV}$  with  $1.3\text{MW}$  of alpha particle heating power.

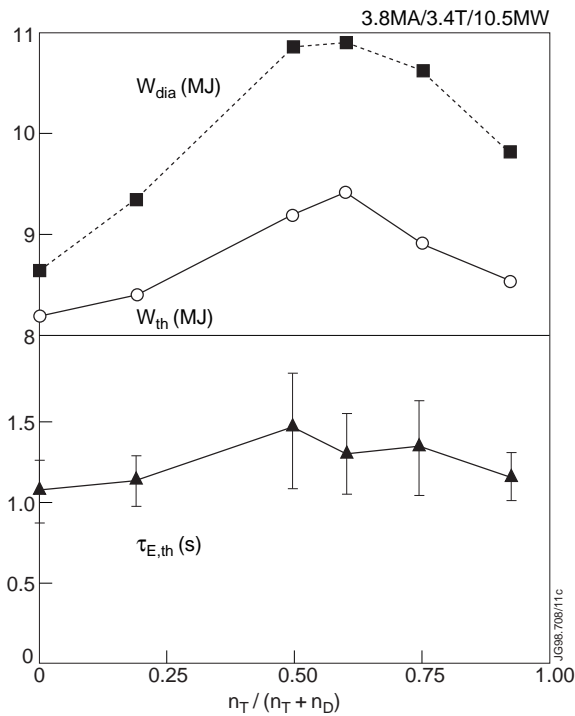


Fig.11 Diamagnetic and thermal plasma energy contents (top) and global energy confinement time (bottom) versus tritium concentrations.

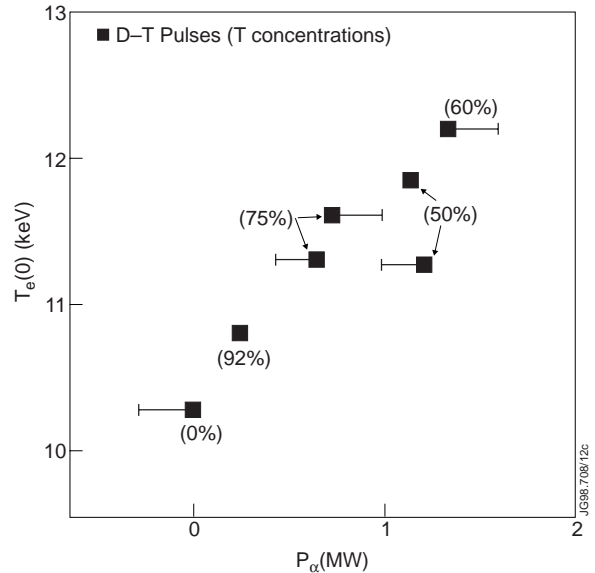


Fig. 12 Central electron temperature versus alpha particle heating power. The bars indicate the variation in NB power compared to the 92% tritium reference pulse. The figures in brackets are the tritium concentrations  $n_T / (n_T + n_D)$ .

These JET experiments are a clear demonstration of the self-heating of a D-T plasma by the alpha particles produced by fusion reactions. A comparison with ICRF heating of deuterium plasmas under similar conditions showed that the alpha particle heating was as effective as hydrogen minority ICRF heating. This is a strong indication that, in the absence of MHD instabilities, the trapping and slowing down of the alpha particles and their heating effect are classical and that there are no unexpected effects which might prevent ignition in a larger device such as ITER.

### 4.3 ICRF heating of D-T plasmas

Ion cyclotron resonance frequency (ICRF) heating is one of the main heating methods foreseen for ITER. During DTE1 the physics and performance of three ICRF schemes applicable to D-T operation ITER and a reactor were tested successfully in steady-state ELMy H-mode discharges [26].

#### 4.3.1 Ion heating schemes

Deuterium minority heating in tritium plasmas, (D)T, at the fundamental resonance of deuterium ( $\omega_{cD}$ ), was demonstrated for the first time on JET [26] and produced strong ion heating. The plasma density and the deuterium minority concentration (up to 20%) were optimised for maximum fusion power from reactions between suprathreshold deuterons and thermal tritons. For a pulse with 9% deuterium and 91% tritium, an ICRF heating power of 6MW generated a steady-state fusion Q of 0.22 for three plasma energy confinement times (2.7s). Doppler broadening of the neutron spectrum showed a deuteron energy of 125keV which was optimum for fusion reactions and close to the critical energy, resulting in strong bulk ion heating ( $T_{i0}=7\text{keV}$  at  $n_{e0}=5\times 10^{19}\text{ m}^{-3}$ ) and high fusion efficiency.

$^3\text{He}$  minority heating, ( $^3\text{He}$ )DT, at the fundamental resonance of  $^3\text{He}$  ( $\omega_{c^3\text{He}}$ ), in approximately 50:50 D:T plasmas with 5-10%  $^3\text{He}$ , also produced strong bulk ion heating. In this case the fusion reactions were thermal with  $T_{i0}\approx T_{e0}=12\text{-}13\text{keV}$ . As discussed below this scheme seems to be the most promising ICRF heating scheme for achieving ignition in ITER.

#### 4.3.2 Electron heating scheme

Heating at the second harmonic of tritium ( $2\omega_{cT}$ ) in a 50:50 D:T plasma produced in JET energetic tritons well above the critical energy and mainly electron heating. The fusion power was mainly from thermal reactions, but was typically a factor of four lower than with  $^3\text{He}$  minority heating under similar conditions.

The central ion and electron temperatures produced in these D-T experiments with the three ICRF heating methods are summarised in Fig. 13.

#### 4.3.3 Code calculations and predictions for ITER

Most of the results obtained in these ICRF heating experiments are in excellent agreement with PION code predictions which gives confidence in the use of these models for predicting ICRF heating in ITER. One result of these predictions is that the  $2\omega_{cT}$  scheme, which preferentially

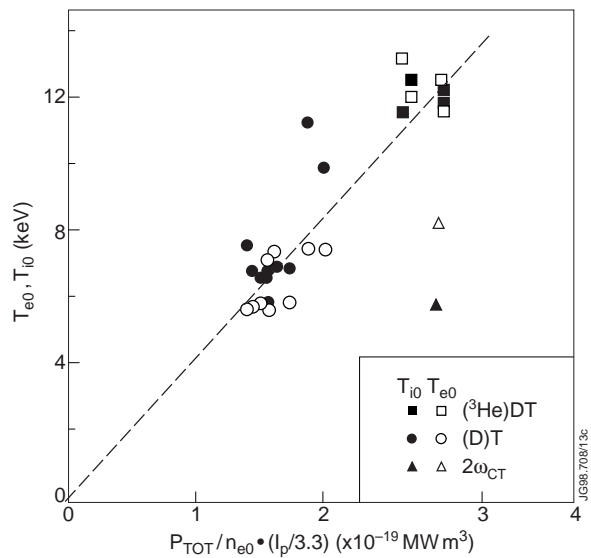


Fig. 13 Central ion and electron temperature plotted against power per particle, corrected for values of plasma current different to 3.3MA.

heats the electrons in JET, will give mainly ion heating in ITER where the power density per particle will be considerably lower resulting in triton tails with lower energies.

The PION code has also been used to investigate the  $^3\text{He}$  minority scheme for ITER [27]. The results for a 2.5% concentration of  $^3\text{He}$  in a 50:50 D:T plasma and a power of 50MW are shown in Fig. 14 in the form of contour plots of constant ion heating fraction in the  $n_{e0}$ ,  $T_{e0}$  space. For illustration a “direct” route from the ohmic ( $T_{e0}=5\text{keV}$ ,  $n_{e0}=3.5\times 10^{19}\text{m}^{-3}$ ) to the ignited phase ( $T_{e0}=35\text{keV}$ ,  $n_{e0}=1\times 10^{20}\text{m}^{-3}$ ) is shown for which the ion heating fraction is larger than 70%, making it an excellent heating scheme for ITER.

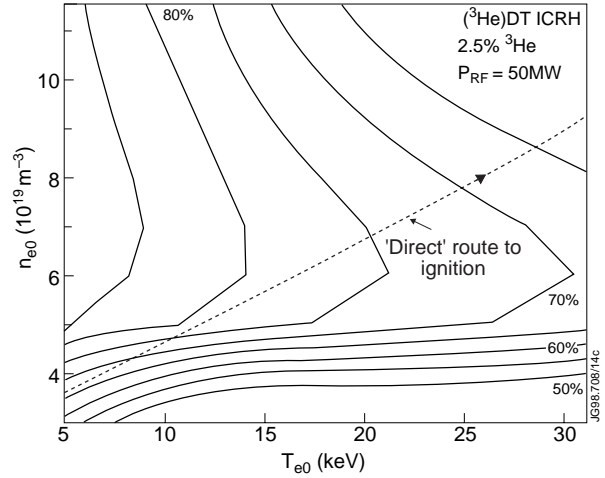


Fig. 14 Contours of constant bulk ion heating fraction for ITER parameters and 2.5%  $^3\text{He}$  minority heating.

#### 4.4 Standard ITER operating mode and extrapolation to ITER

##### 4.4.1 Mass scaling of H-mode threshold power

The effect of isotope mass on the heating power needed to access the H-mode regime was studied during DTE1 in a series of experiments which included discharges with  $\approx 60\%$  and  $\approx 90\%$  tritium concentrations in deuterium. The most notable result was that, in comparison with previous experiments in pure deuterium, the H-mode threshold power was lower in D-T and lower still in pure tritium, roughly as the inverse of the atomic mass ( $A^{-1}$ ). This can be seen in Fig. 15 which shows the loss power from the plasma plotted as a function of the scaling  $P_{\text{Th}}=0.76 \bar{n}_e^{0.75} B R^2 A^{-1}$ , which has been modified from that used for ITER [28] by the inclusion of an inverse mass dependence (the constant of proportionality has been adjusted to give the best fit to these JET data). Following DTE1, similar experiments were carried out in hydrogen, and these data are also shown in Fig. 15, and confirm the strong inverse mass dependence.

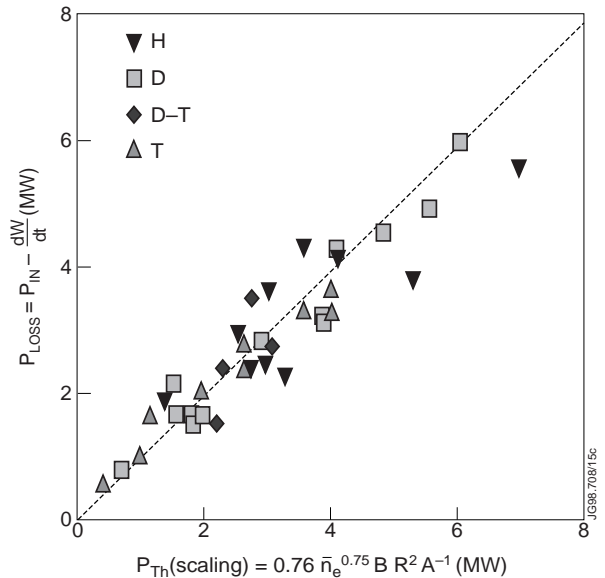


Fig. 15 Plasma loss power for ELMy H-mode discharges in hydrogen, deuterium, deuterium-tritium and tritium plotted against the ITER scaling for the H-mode threshold power modified to include an inverse mass dependence.



start-up phase) and a 20% reduction in the power needed to access or stay in the H-mode in a 50:50 D:T mixture. These results are very favourable for ITER, leading to increased operational flexibility.

#### 4.4.2 Mass dependence of energy confinement in ELMy H-modes

The most recent version of the multi-machine data base for steady state ELMy H-mode discharges shows that the global energy confinement time scales as  $A^{0.2}$  with mass (the ITERH-97(y) scaling [29] which is used at present for extrapolation to ITER). Before, during and after DTE1, steady state ELMy H-modes were obtained for a wide range of plasma currents (1-4.5MA) and toroidal fields (1-3.8T) in hydrogen, deuterium, D-T and tritium. The energy confinement times in these discharges were found to be consistent with the ITERH-97(y) scaling, with its  $A^{0.2}$  dependence providing an acceptable fit (Fig. 16). However, a more refined analysis shows that a better fit is with practically no mass dependence ( $A^{0.03\pm 0.1}$ ).

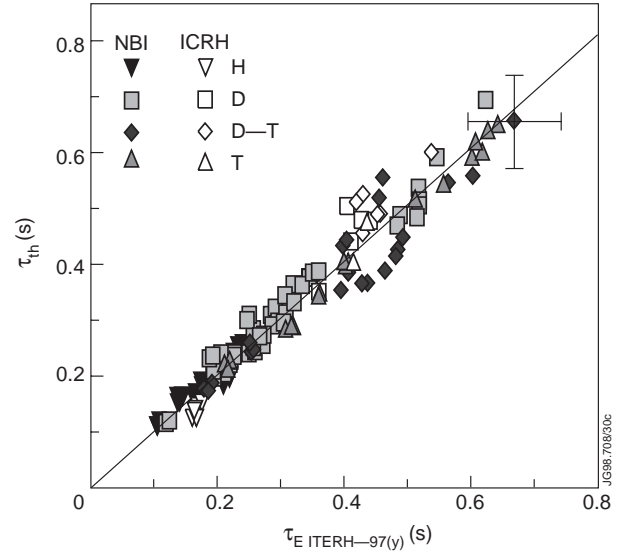


Fig. 16 Measured thermal energy confinement times in hydrogen, deuterium, deuterium-tritium and tritium ELMy H-mode discharges plotted against the ITER scaling law.

This result presents a challenge to theoretical understanding which can be resolved by separating the total stored plasma energy into two components which scale differently with respect to mass (and other significant parameters). The first component is the pedestal energy (Fig. 17(a)) which is determined from the edge density and temperature (assuming equal electron and ion temperatures), and which shows a strong mass dependence. The data shown is fitted by an  $A^{0.5}$  dependence which would result, for example, from the gradient of the plasma pressure being limited in the edge by ideal ballooning mode instabilities over a distance characterised by the Larmor radius of ions [30]. The second component is the core energy which is determined by subtracting the pedestal energy from the total thermal plasma energy. The corresponding thermal core energy confinement time (Fig. 17(b)) is found to scale as  $A^{-0.17\pm 0.1}$ , consistent with the  $A^{-0.2}$  mass dependence which would be expected from a gyro-Bohm scaling, generic of theoretical transport models based on turbulence with a scale length of the ion Larmor radius.

These differences between the edge and core transport are confirmed by local transport analysis [31] which shows the core transport data to be consistent with gyro-Bohm scaling. This is a very significant result since for the first time energy transport in the plasma core can be



related to gyro-Bohm scaling, including its implicit mass dependence. It also emphasises that the large size of JET makes its data particularly valuable for separating core and edge effects in the global energy balance.

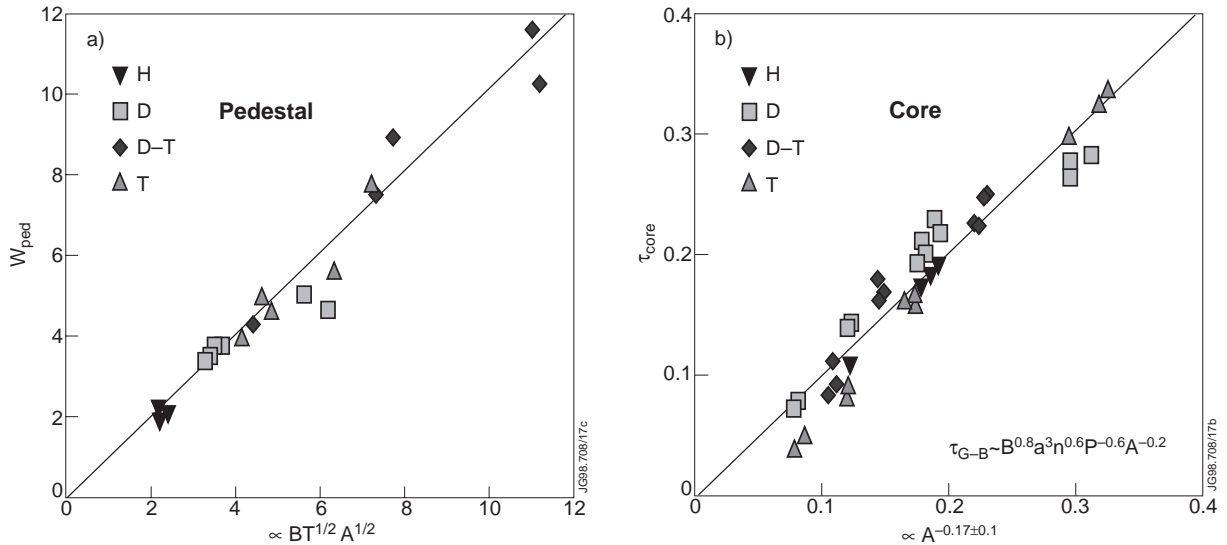


Fig. 17 (a) Pedestal energy plotted against that expected from an edge pressure gradient limited by ballooning modes over an ion poloidal Larmor radius and (b) the thermal confinement time of the core plasma plotted against the best fit for the mass dependence in a pure gyro-Bohm scaling for ELMy H-mode discharges in hydrogen, deuterium, deuterium-tritium and tritium.

#### 4.4.3 ITER demonstration pulses and extrapolation to ITER

During DTE1 the best ever fusion performance in an ITER-like H-mode was obtained in a 3.8MA/3.8T discharge which was maintained in steady-state by regular Type I ELMs. This resulted in the production of a fusion energy of 21.7MJ, a ratio of the fusion energy produced to the input energy of 0.18 over 3.5s ( $\approx 8$  energy confinement times) and 4MW of fusion power being maintained for  $\approx 4$ s (see Fig. 10).

The normalised plasma pressure, being limited to  $\beta_N=1.3$  by the available additional heating power (23MW of combined NB (90%) and ICRF (10%) heating), was too low for these discharges to qualify as ITER demonstration pulses. However, at lower toroidal field and plasma current (e.g. at 2MA/2T) the normalised plasma pressure ( $\beta_N=2.2$ ) and collisionality of an ignited ITER were matched on JET and the edge safety factor was also close to the ITER value ( $q=3.2$ ). The characteristic signals of such a discharge in D-T are shown in Fig. 18; it forms the basis for a series of “wind tunnel” experiments which preserve on JET all relevant dimensionless parameters close to ITER values, except for the normalised plasma size,  $\rho^* = \rho_i/a$  (with  $\rho_i$  the ion Larmor radius and  $a$  the plasma radius). The data from this series of experiments is shown in Fig. 19 to scale close to gyro-Bohm, extrapolating to ignition in ITER. In fact, a gyro-Bohm extrapolation from this ITER demonstration pulse gives ignition at 1.8GW (or  $Q=5.8$  for a Bohm extrapolation) for ITER operating at 21MA. The required density would, however, be 50% above the Greenwald density limit, and confinement in JET and other tokamaks is degraded as this

high density limit is approached (see Fig. 7(a)). However, it has been possible to extend the ITER demonstration pulses to ITER operation at the higher plasma current of 24MA (and correspondingly lower  $q_{05}=2.76$ ). In this case, ignition is predicted at the 1.05GW level for a gyro-Bohm extrapolation (or  $Q=7.3$  for a Bohm extrapolation), but the required density is now lower and close to the Greenwald density.

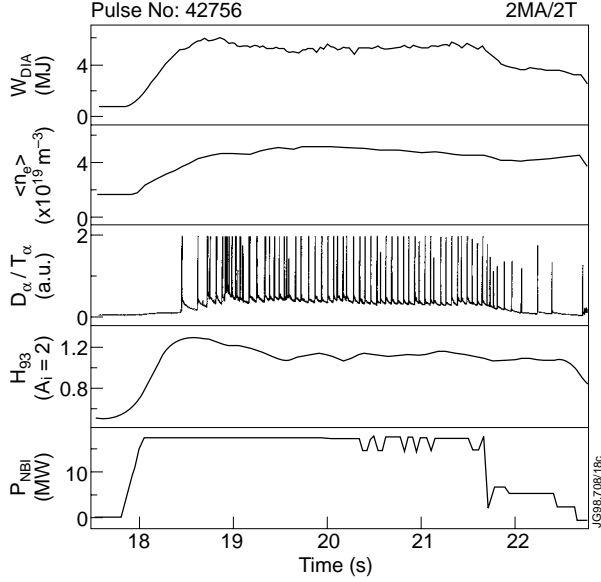


Fig. 18 Steady-state ELMy H-mode with ITER collisionality and normalised plasma pressure ( $\beta_N=2.4$ ) in D-T. Basis for “Wind Tunnel” experiments in JET.

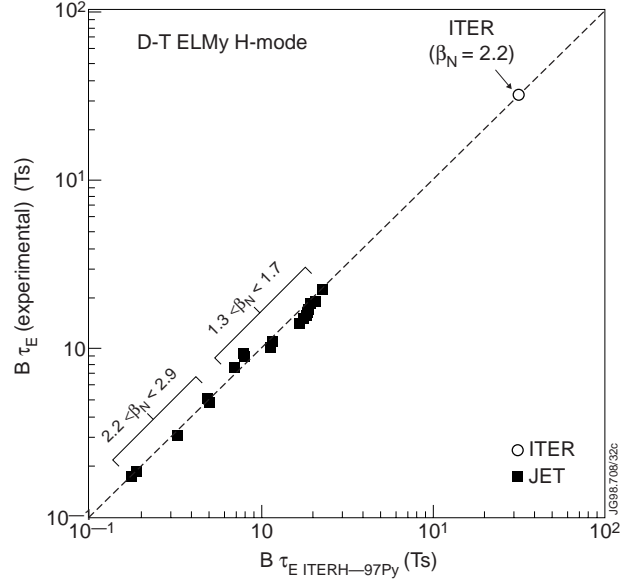


Fig. 19 Measured thermal energy confinement times of ITER similarity ELMy H-mode discharges in D-T plotted against the scaling law used in ITER projections. The operating point of an ignited ITER is also shown.

## 5. ADVANCED TOKAMAK SCENARIOS

Advanced tokamak concepts propose the use of profile control techniques to increase fusion performance and to develop these conditions into steady-state by driving a large fraction of the plasma current non-inductively. This concept, if successful, would give ignition and sustained burn at lower plasma current, thereby reducing the size and cost of a fusion reactor. Fusion power,  $P_{\text{fus}}$ , and bootstrap current fraction,  $I_{\text{BS}}/I$ , are given by

$$P_{\text{fus}} \approx \beta_t^2 B^4 V \approx \beta_N^2 I^2 B^2 R \kappa \quad (1)$$

$$\frac{I_{\text{BS}}}{I} \approx \epsilon^{1/2} \beta_p \approx \frac{\beta_N B \kappa a \epsilon^{1/2}}{I} \quad (2)$$

Obviously high magnetic field  $B$ , and elongation  $\kappa$ , are beneficial in this context, while the plasma current  $I$ , has to be chosen as a compromise between fusion power and bootstrap current fraction, and can be the lower, the higher  $\beta_N$  is made. In practical terms,  $\beta_p \geq 2$  and  $\beta_N \geq 3$  are considered minimum requirements for  $I_{\text{BS}}/I \approx 80\%$  and significant fusion power (e.g. to obtain 1GW at 12-13MA in ITER).

Plasma pressure peaking and current profile modifications have led to enhanced performance as will be demonstrated in the following for the Pellet-Enhanced-Performance (PEP) mode and the optimised shear mode.

## 5.1 Pellet-enhanced-performance mode (1988)

The first observation of reversed magnetic shear behaviour was recorded in JET in the PEP-mode of 1988 [32-34]. Pellet injection to the plasma core created transiently a large central region (about 40% of the minor radius) with slightly negative (reversed) magnetic shear (Fig. 20(a)) [33] due to the combined effects of a transient inversion of the temperature and consequently current density profile, and a substantial bootstrap current driven by the density gradient. This resulted in centrally peaked density and temperature profiles (Fig. 20(b)) and a reduction in particle and energy transport (electrons and ions) close to neoclassical levels (Fig.20(c)). The enhanced performance of the reversed shear plasma manifested itself in strongly increased neutron rates

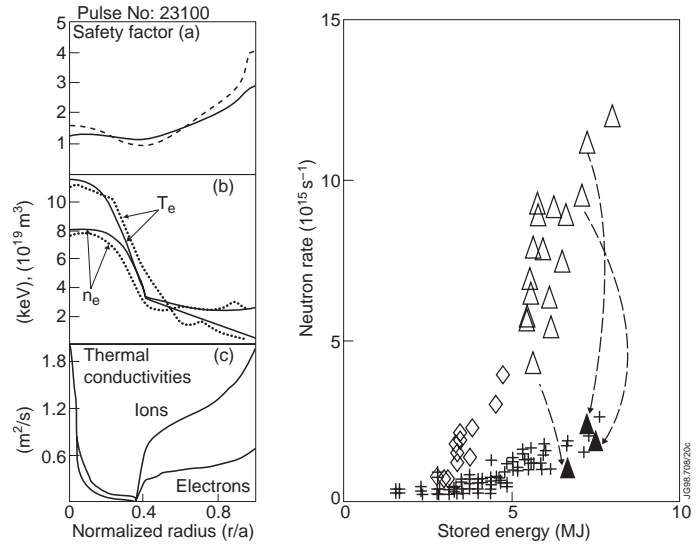


Fig. 20 (a), (b) and (c) show results of a PEP pulse simulation obtained with a time dependent 1-D transport Code (solid curves). (a)  $q$ -profile (dashed curve calculated by IDENTD), (b) electron temperature and density profiles (dotted curves are LIDAR measurements), (c) ion and electron thermal conductivities. (d) shows neutron rates versus stored energy for various types of PEP mode discharges.  $\Delta$  and  $s$  represent PEP mode data at maximum neutron rate and after decay of pellet enhancement, respectively. For comparison, standard H-mode (+) and limiter PEP L-mode ( $\diamond$ ) data are also shown.

(about a factor of 10 compared to standard H-mode, Fig. 20(d)) [34] which reverted back to H-mode levels after the collapse of the reversed shear configuration. The PEP-mode was the first manifestation in a tokamak that plasma confinement and stability can be improved by modifying the current density profile.

## 5.2 Optimised shear mode (since 1996)

### 5.2.1 Formation of internal transport barriers

A key element of optimised (reversed) shear modes [35-39] is the formation of an internal transport barrier (ITB) and these have now been established for the first time in D-T [40]. Power and current profile control are used to establish an ITB, to delay the transition to an H-mode phase, and to avoid a  $\beta$  limit disruption [35,36]. The scenario comprises the formation of a target plasma by pre-heating during a fast current ramp, using lower hybrid waves to assist breakdown and to provide some current drive, followed by ICRF pre-heating to arrest current penetration. When the current profile is such that the volume within the  $q=2$  surface is reasonably large ( $r/a \approx 0.3-0.4$ ),

the full heating power, typically 16-18MW of NB heating together with 6MW of ICRF heating, is applied (Fig. 21). In D-D plasmas, the highest fusion performance has been obtained when a clear H-mode transition was delayed for as long as possible. When an ITB is established, the resulting good core confinement maintains, at least transiently, the plasma loss power below the level required to trigger an H-mode, thus preserving an L-mode edge.

In D-T plasmas, the scenario had to be modified, largely because of the lower H-mode threshold power [41, 24]. However, after some scenario development, strong ITBs were established for the first time in D-T plasmas, and with a threshold heating power and current profiles not markedly different from those in D-D plasmas [37]. When an ITB forms, substantial increases in plasma density and temperature (Fig. 22) occur: temperature gradients can reach

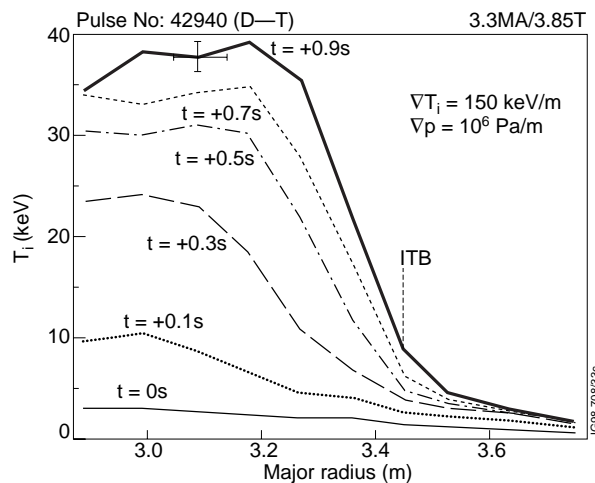


Fig. 22 Ion temperature profiles at various times after the start of high power heating in an optimised shear discharge showing the formation of an internal transport barrier (ITB).

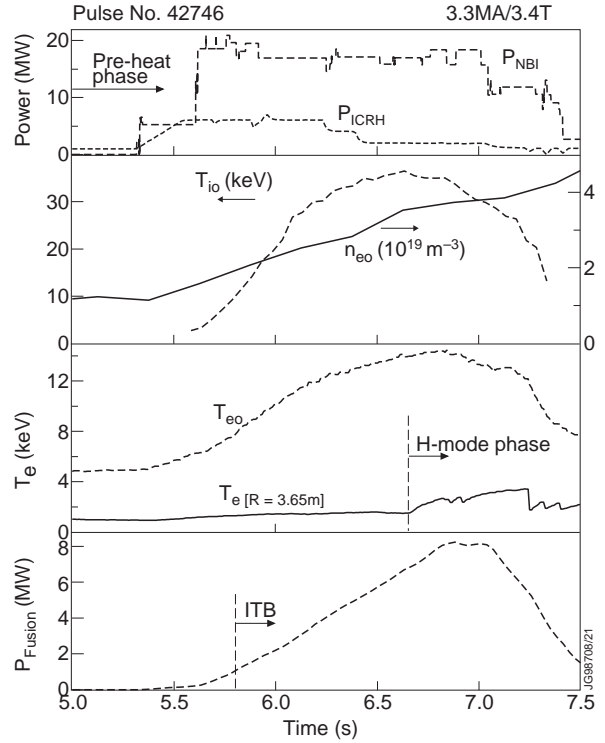


Fig. 21 Various time traces for the optimised shear discharge with the highest fusion yield. From top to bottom: NB and ICRF input power; central ion temperature and electron density; central and edge ( $R=3.65m$ ) electron temperature; and fusion power.

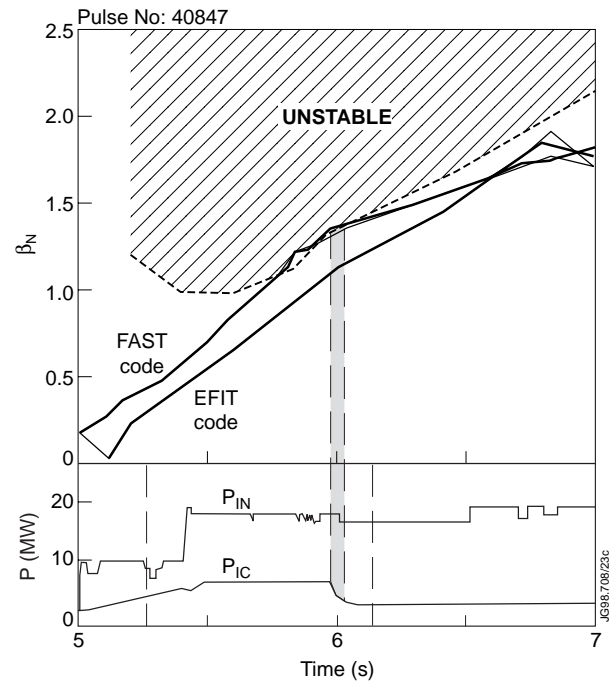


Fig. 23 Normalised plasma pressure as function of time during a high performance optimised shear discharge. By controlling the heating power the discharge avoids the region unstable to  $n=1$  kink modes.

150keV/m and pressure gradients 1MPa/m. In these discharges the input power is controlled by feedback on the neutron rate in order to avoid excessive pressure gradients which provoke MHD instabilities. As a result, the plasma can be maintained close to the ideal MHD stability limit for most of the heating pulse, as shown in Fig. 23 for an optimised shear discharge in D-D [42].  $\beta_N$  increases as the ITB moves outwards with time to  $\approx 2/3$  of the plasma radius and the pressure profile becomes less peaked. The highest performance has been achieved with small or slightly reversed central shear and  $q(0)$  in the range 1.5-2.

This is confirmed by TRANSP simulations, which also show that more than half of the plasma current at peak performance was driven non-inductively. Furthermore, the TRANSP calculations show that the ion thermal diffusivity can be very low and approaches neoclassical values within the ITB, both in D-D and D-T plasmas, as shown in Fig. 24 [40]. The neutron and time constraints on DTE1 did not allow these discharges to be optimised. Nevertheless, 8.2MW of fusion power was produced (Fig. 21).

### 5.2.2 Simultaneous internal and edge transport barriers and development towards steady-state

The highest fusion performance was normally obtained by prolonging the phase during which the plasma edge was in L-mode [35,36]. A significant number of discharges, however, developed both an ITB and an ELMy H-mode edge [19], as illustrated in Fig. 25, with a substantial fusion yield being produced. In the discharge shown in Fig. 25, an ITB is formed and the central ion temperature reaches 24keV, while the edge ion temperature is about 3keV, typical of an ELMy H-mode.

In this pulse the fusion power increases from the start of the main heating phase until it reaches 6.8MW, at which time the input power was reduced to economise on D-T neutrons. This increase in fusion yield is due to a continuous build-up of central density together with an increase of the tritium concentration. The stored plasma energy reaches 8.8MJ for a total injected power of 18.4MW and a corresponding confinement enhancement factor  $H_{89} \approx 2.3$  relative to the ITER89-P scaling [43]. In this pulse, as in similar D-T and D-D pulses, the positions of the  $q=2$  magnetic surface and the ITB change only slowly with time as a result of the generation of an edge bootstrap current.

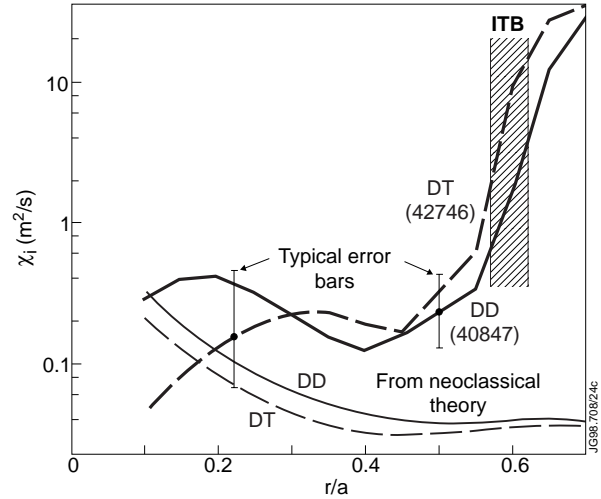


Fig. 24 Ion thermal diffusivities versus normalised plasma radius for two optimised shear discharges in D-D and D-T and comparison with neoclassical values.

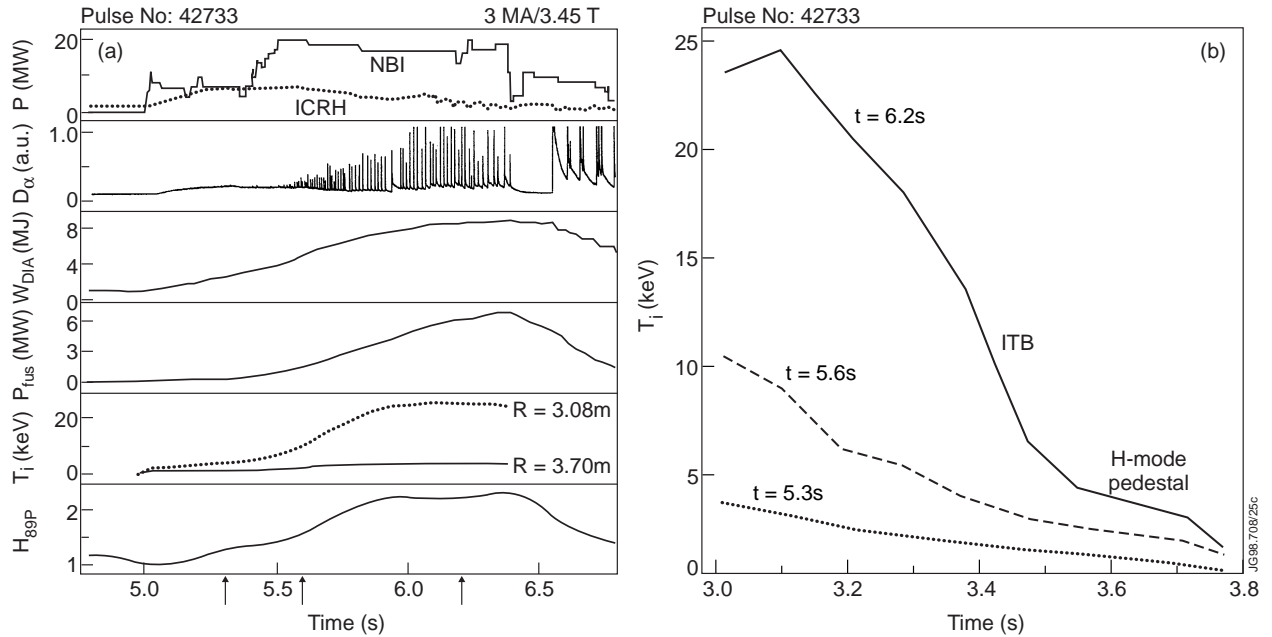


Fig. 25 (a) Various time traces and (b) ion temperature profiles for a pulse which develops an internal transport barrier simultaneously with an ELMy H-mode barrier.

An additional interesting feature of these double barrier discharges is that they have much smaller ELM amplitudes than conventional ELMy H-mode discharges [44]. This could alleviate the problem of the critically high peak power loads on the divertor targets in a standard ELMy H-mode ignited ITER scenario.

This route, which could not be explored further during DTE1 due to the imposed constraint on the neutron budget, shows significant promise for steady-state high fusion yield D-T plasmas, but would require a technique for better control of the plasma edge and/or current profile.

## 6. SUMMARY AND CONCLUSIONS

JET is a unique step on the way to a fusion reactor, demonstrating considerable synergy between physics and engineering. The large size of JET allows operation under conditions closest to a Next Step tokamak. The flexibility of the design has made machine modifications and upgrades possible within reasonable time and costs. This has allowed high power operation in limiter and X-point configurations, with different plasma facing materials and in different modes of tokamak operation. In high confinement H-mode operation in deuterium, plasma parameters in JET have reached values which, if reproduced in a D-T plasma, would constitute break-even (JET's progress in performance over the years is shown in Fig. 26). In addition, the large flexibility of the JET design has made possible the installation of a series of progressively more closed divertors which have allowed significant contributions to the development of a divertor concept for ITER and a reactor.

The D-T and Remote Handling capabilities of JET formed the basis for a number of unique results in D-T: the first significant controlled production of fusion power in 1991; the record



fusion powers and the first clear observation of alpha particle heating in 1997; the validation of ICRF heating schemes in D-T; the more accurate assessments of the heating requirements and ignition margin for ITER; and finally the Remote Handling installation of the Mark IIGB divertor in 1998, thereby demonstrating a key technology for ITER and a reactor.

JET has still much to offer the European and world fusion programmes. With its unique combination of divertor configuration, heating and profile control systems and tritium capability, JET will remain, for many more years, the most valuable machine in support of ITER or any other Next Step tokamak.

## ACKNOWLEDGEMENTS

The author wishes to thank all his colleagues at JET who have made these significant achievements possible and in particular J.G. Cordey, C. Gormezano, P.J. Lomas, F.X. Söldner, D.F. Start and P.R. Thomas for material presented in this paper. He would like to give special credit to M.L. Watkins for his help in preparing this paper.

## REFERENCES

- [1] M.A. Pick and the JET Team, The technological achievements and experience at JET, Paper IN19, this conference.
- [2] R. Aymar, V. Chuyanov, M. Huguet, R. Parker, Y. Shimomura and the ITER Joint Central Team and Home Teams, in Fusion Energy 1996 (Proc. 16th Int. Conf. Montreal, Canada, 1996) Vol. 1, IAEA, Vienna (1997) 3.
- [3] JET Team (presented by P.H. Rebut), Plasma Phys. Contr. Nucl. Fus. Res. 1986, Vol. I, IAEA, Vienna (1987) 31.
- [4] R.J. Goldston, Energy confinement scaling on tokamaks, Plasma Physics, Vol.26, No.1A (1984) 87.
- [5] F. Wagner et al., Phys. Rev. Letters, **49** (1982) 1408.
- [6] A. Tanga et al., in Plasma Phys. and Contr. Nucl. Fus. Res. 1986 (Proc. 11th Int. Conf. Kyoto, 1986), Vol. I, IAEA, Vienna (1987) 65.
- [7] JET Team (presented by P.H. Rebut), Plasma Phys. and Contr. Nucl. Fus. Res. 1990 (Proc. 13th Int. Conf. Washington, US, 1990), Vol. I, IAEA, Vienna (1991) 27.

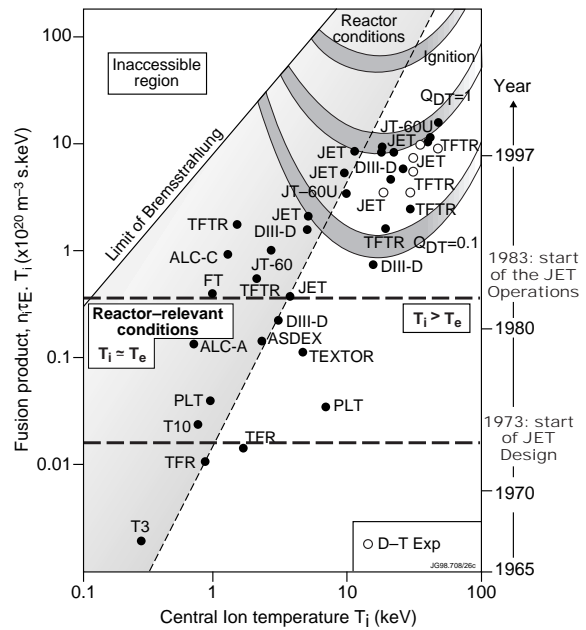


Fig. 26 Fusion triple product versus central ion temperatures showing progress in fusion performance since the start of JET design work in 1973.

- [8] JET Team, Nucl. Fusion **32** (1992) 187.
- [9] P-H. Rebut et al., Fus. Eng. Design **22** (1993) 7.
- [10] JET Team (presented by G.C. Vlases), in Fusion Energy 1996 (Proc. 16th Int. Conf. Montreal, Canada, 1996) Vol. 2, IAEA, Vienna (1997) 371.
- [11] L.D. Horton et al., Studies in JET divertors of varied geometry I: non seeded plasma operation, report JET-P(98), accepted for publication in Nucl. Fusion.
- [12] G.M. McCracken et al., Nucl. Fusion **38** (1998), accepted for publication in Nucl. Fusion.
- [13] M. Greenwald et al., Nucl. Fusion **28** (1988) 2199.
- [14] G.F. Matthews et al., Studies in JET divertors of varied geometry II: impurity seeded plasmas, report JET-P(98)20, accepted for publication in Nucl. Fusion.
- [15] S. Putvinski et al., in Fusion Energy 1996 (Proc. 16th Int. Conf. Montreal, Canada, 1996) Vol. 2, IAEA, Vienna (1997) 737.
- [16] P.T. Lang et al., to be published in Proc. 25th Europ. Conf. on Controlled Fusion and Plasma Physics, Prague, Czech Rep., 29 June - 3 July 1998, by Eur. Phys. Soc., Geneva (1998).
- [17] JET Team, (presented by R.D. Monk), Paper IAEA-CN-69/Exb/4, IAEA Conf., Yokohama, Oct. 1998.
- [18] A. Gibson and the JET Team, Physics of Plasmas **5** (1998) 1839.
- [19] M. Keilhacker et al., and the JET Team, "High Fusion Performance from Deuterium-Tritium Plasmas in the JET Tokamak", to appear in Nucl. Fusion (February 1999).
- [20] JET Team (presented by P. J. LOMAS), in Fusion Energy 1996 (Proc. 16th Int. Conf. Montreal, Canada, 1996) Vol. 1, IAEA, Vienna (1997) 239.
- [21] M.F.F. Nave et al., Nucl. Fusion **37** (1997) 809.
- [22] F. B. Marcus et al., Nucl. Fusion **33** (1993) 1325.
- [23] K. M. McGuire et al., in Fusion Energy 1996 (Proc. 16th Int. Conf. Montreal, Canada, 1996) Vol. 1, IAEA, Vienna (1997) 19.
- [24] J. Jacquinot et al., and the JET Team, "Overview of ITER Physics D-T Experiments in JET " to appear in Nucl. Fusion (February 1999).
- [25] P. R. Thomas et al., Phys. Rev. Lett. **80** (1998) 5548.
- [26] D.F.H. Start et al., Phys. Rev. Lett. **80** (1998) 4681.
- [27] D.F.H. Start et al., in Europhysics Conference Abstracts (Proc. of the 24th EPS Conference on Controlled Fusion and Plasma Physics, Berchtesgaden, Germany, 1997), Vol 21A, Part 1, 141.
- [28] ITER Confinement Database and Modelling Expert Group (presented by T. Takizuka), in Fusion Energy 1996 (Proc. 16th Int. Conf. Montreal, Canada, 1996) Vol. 2, IAEA, Vienna (1997) 795.
- [29] ITER Confinement Database and Modelling Working Group, presented by J.G. Cordey, Plasma Phys. Control. Fusion **39** (1997) B115.



- [30] JET Team (presented by M. Keilhacker), Plasma Phys. Control. Fusion **39** (1997) B1.
- [31] R.V. Budney et al., to be published in Proc. 25th Europ. Conf. on Controlled Fusion and Plasma Physics, Prague, Czech Rep., 29 June - 3 July 1998, by Eur. Phys. Soc., Geneva (1998).
- [32] JET Team (presented by J. Jacquinot), Plasma Phys. Control. Fusion **30** (1988) 1467.
- [33] M. Hugon et al., Nucl. Fusion **32** (1992) 33.
- [34] B.J.D. Tubbing et al., Nucl. Fusion **31** (1991) 839.
- [35] JET Team (presented by C. GORMEZANO), in Fusion Energy 1996 (Proc. 16th Int. Conf. Montreal, Canada, 1996) Vol.1, IAEA, Vienna (1997) 487.
- [36] JET Team (presented by F. X. SÖLDNER), Plasma Phys. Control. Fusion **39** (1997) B353.
- [37] C. Kessel et al., Phys. Rev. Lett. **72** (1994) 1212.
- [38] E. J. Strait et al., Phys. Rev. Lett. **75** (1995) 4421.
- [39] K. Ushigusa and the JT-60 Team, in Fusion Energy 1996 (Proc. 16th Int. Conf. Montreal, Canada, 1996) Vol.1, IAEA, Vienna (1997) 37.
- [40] C. Gormezano et al., Phys. Rev. Lett. **80** (1998) 5544.
- [41] JET Team (presented by M. KEILHACKER), Plasma Phys. Control. Fusion **39** (1997) B1.
- [42] G.T.A.Huysmans et al., 24th Europ. Phys. Soc. Conf. on Controlled Fusion and Plasma Physics Berchestgaden, Germany, 1997 Vol. 21A, Part 1, 21.
- [43] D.P. Schissel et at., Nucl. Fusion **31** (1991) 73.
- [44] F.X. Söldner et al., "Approach to Steady-State High Performance in DD and DT with Optimised Shear in JET", submitted for publication in Nucl. Fusion (1999).